ORIGINAL ARTICLE

Journal of Applied Microbiology

Antifungal activity of 2-chloro-N-phenylacetamide, docking and molecular dynamics studies against clinical isolates of *Candida tropicalis* and *Candida parapsilosis*

Shellygton Lima Silva[1] 🟢 | **Fillipe de Oliveira Pereira**[2] | **Laisa Vilar Cordeiro**[1] | **Hermes Diniz Neto**[1] | **Mayara dos Santos Maia**[1] | **Helivaldo Diogenes da Silva Souza**[3] | **Petrônio F. de Athayde-Filho**[3] | **Marcus Tullius Scotti**[1] | **Luciana Scotti**[1] 🟢 | **Edeltrudes de Oliveira Lima**[1]

[1]Postgraduate Program in Natural and Bioactive Synthetic Products, Department of Pharmaceutical Sciences, Federal University of Paraiba, João Pessoa, Paraíba, Brazil

[2]Biochemistry Laboratory, Academic Unit of Health, Education and Health Center, Federal University of Campina Grande, Cuité, Paraíba, Brazil

[3]Bioenergy and Organic Synthesis Research Laboratory, Department of Chemistry, University of Paraiba, João Pessoa, Paraíba, Brazil

Correspondence
Shellygton Lima Silva, Postgraduate Program in Natural and Bioactive Synthetic Products, Federal University of Paraiba, João Pessoa, Paraíba, Brazil.
Email: shellygton@hotmail.com

Funding information
CNPq; CAPES; Federal University of Paraíba

Abstract

Aims: This study evaluated the antifungal, antibiofilm and molecular docking of 2-chloro-N-phenylacetamide against clinical isolates of *Candida tropicalis* and *Candida parapsilosis*.

Methods and results: Minimum inhibitory concentration (MIC) of the test drugs was determined by microdilution. A1Cl obtained MIC values ranging from 16 and 256 μg/ml. Fluconazole MIC ranging from 16 and 512 μg/ml. MIC of A1Cl showed fungicide activity, emphasizing the solid antifungal potential of this drug. An association study was performed with A1Cl and fluconazole (checkerboard), revealing indifference by decreasing. Thus, we conducted this study using A1Cl isolated. In the micromorphological assay, the test drugs reduced the production of virulence structures compared to the control (concentration-dependent effect). A1Cl inhibited in vitro biofilm formation at all concentrations tested ($1/4$MIC to $8 \times$ MIC) ($p < 0.05$) and reduced mature biofilm biomass ($p < 0.05$) against *C. tropicalis* and *C. parapsilosis*. In the ex vivo biofilm susceptibility testing (human nails fragments), A1Cl inhibited biofilm formation and reduced mature biofilm biomass ($p < 0.05$) more than 50% at MIC. Fluconazole had a similar effect at $4 \times$ MIC. In silico studies suggest that the mechanism of antifungal activity of A1Cl involves the inhibition of the enzyme dihydrofolate reductase (DHFR) rather than geranylgeranyltransferase-I.

Conclusions: The results suggest that A1Cl is a promising antifungal agent. Furthermore, this activity is related to attenuation of expression of virulence factors and antibiofilm effects against *C. tropicalis* and *C. parapsilosis*.

KEYWORDS
antibiofilm, onychomycosis, resistance, synthetic drug

INTRODUCTION

Onychomycosis is a chronic fungal infection of the nails caused by dermatophytes, non-dermatophyte moulds and yeasts (Gupta et al., 2020). It causes discoloration, thickening, fragility and eventual nail bed separation (Andrés & Alexandro, 2020). Over the years, *Candida parapsilosis* has been the most common *Candida* species for infections of the fingers and toes (Kukhar et al., 2020), and *C. tropicalis* (Arrua et al., 2015) has emerged as the second-line pathogen causing onychomycosis (Torres-Guerrero & Arenas, 2017).

Onychomycosis is the most common nail disease worldwide. It affects approximately 5.5% of the population worldwide, predominately older people over younger people (Lipner & Scher, 2019). Onychomycosis development is often associated with several factors, such as chronic exposure to the fungi, use of antibiotics or immunosuppressive medications, diabetes mellitus, HIV–AIDS and peripheral venous insufficiency (Andrés & Alexandro, 2020).

Usually, systemic therapy involving a broad spectrum is required to achieve higher cure rates in managing onychomycosis by Candida. Triazoles (fluconazole and itraconazole) are the most systemic antifungal drugs currently in use. However, they have limitations, such as hepatotoxicity and drug interactions (Gupta et al., 2020).

Onychomycoses are difficult-to-treat mycoses with a high recurrence rate and require an extended duration of treatment. In part, it occurs due to resistance mechanisms developed by *Candida*, such as biofilms. Biofilms are microbial communities adhered to surfaces, such as nail plates characterized by producing an extracellular polymeric matrix that promotes fungus adhesion, protection against antifungal drugs, and supports the differential expression of genes related to fungal virulence (Gupta, Jessie, et al., 2018; Nett & Andes, 2020). In this context, the development of new antifungals is a critical topic.

These challenges drive studies to obtain new effective drugs against fungal biofilms targeting molecular targets in *Candida*. Literature reports have shown an interest in prospective studies with substitutions in acetanilide derivatives. This group, present in several synthetic drugs, is related to antibacterial, antiviral, antifungal and anti-inflammatory activities (Cordeiro et al., 2020). Previous studies confirm the antimicrobial potential of acetamide derivatives. Yurttaş et al. (2020) demonstrated that the combination of 2-chloro-N-(substituted[benzo]/thiazole) acetamide derivatives with hydroxyquinoline yielded more active molecules. Shinde et al. (2020) used benzothiazole and piperazine to synthesize an acetamide derivative with marked antifungal activity against *C. albicans* and *A. fumigatus*.

Synthetic chloroacetamide derivatives are promising drugs because they demonstrate anticancer (Khazir et al., 2020), antibacterial (Cordeiro et al., 2020; Yadav et al., 2018) and antifungal (Melo et al., 2020) activity. Furthermore, there are no available studies on the antifungal effects of chloroacetamides against clinical isolates of *C. tropicalis* and *C. parapsilosis*. Therefore, further exploration of these properties is necessary.

In this context, the generation of new antifungals is an urgent topic. Our study presents 2-chloro-N-phenylacetamide (A1Cl) as a new synthetic fungicide against *C. tropicalis* and *C. parapsilosis* strains. In addition, we investigated its antifungal potential with particular emphasis on the antibiofilm effect. Based on molecular docking and molecular dynamics studies, we also proposed the enzyme dihydrofolate reductase (DHFR) as a possible molecular target of action. DHFR is a crucial enzyme in the folic acid metabolic pathway, which plays an essential role in cell proliferation and growth (Joshi et al., 2021). Then, it may be a differential factor in the involvement and severity of onychomycosis caused by *Candida*.

MATERIALS AND METHODS

Fungal strains

The following clinical isolates were used: *C. tropicalis* ATCC-13809, LM-98, LM-111, LM-135 and *C. parapsilosis* ATCC-22019, LM-78, LM-197 and LM-707. These fungi belong to the fungal culture collection of the Laboratory of Mycology (Federal University of Paraíba, Brazil). The fungi were cultivated in Sabouraud dextrose agar (Difco®) at 28°C for 48 h to obtain the fungal inocula in a sterile saline solution (0.85% NaCl). The turbidity of the final inoculum has been adjusted to the McFarland standard 0.5 scales (1.5×10^6 CFU ml) (Clinical and Laboratory Standards Institute, 2017).

Antifungal susceptibility testing

Fluconazole (Sigma-Aldrich®) was used in this study as a standard drug. The Bioenergy and Organic Synthesis Research Laboratory (Federal University of Paraíba, Brazil) synthesized 2-chloro-N-phenylacetamide (A1Cl) (Souza et al., 2019). Initially, we solubilized the drugs in dimethyl sulfoxide (DMSO; Sigma-Aldrich®). Then, we made dilutions to reach 1 µg/ml using RPMI 1640 medium (Sigma-Aldrich®). Next, we determined the minimum inhibitory concentration (MIC) of fluconazole and A1Cl against the *Candida* strains by microdilution, using

in RPMI 1640 (Sigma-Aldrich®; Clinical and Laboratory Standards Institute, 2017). Finally, we performed controls for sterility, cell viability and DMSO at 5%. MIC is defined as the lowest concentration capable of causing complete inhibition of fungal growth visually after 48 h at 35 ± 2°C. After MIC determination, an aliquot of 10 μl from the wells with no fungal growth was transferred to other plate containing RPMI-1640 to determine the minimum fungicidal concentration (MFC) (Ferreira et al., 2021). The plates were incubated at 48 h at 35 ± 2°C. MFC was determined after the incubation time as the lowest concentration in which no fungal growth was observed.

Study of association between drugs

The effect of the association of A1Cl with the fluconazole was analysed by checkerboard technique (Lewis et al., 2002). We prepared dilutions of the test drug solutions at 1/8MIC, 1/4MIC, 1/2MIC, MIC, 2 × MIC 4 × MIC and 8 × MIC in RPMI 1640. An aliquot of 50 μl of fluconazole was then added to the wells of the plate in a vertical sense, and then 50 μl of a specific A1Cl dilution was added in the horizontal direction of the plate. Finally, 100 μl of inoculum was added. The plates were sealed and incubated at 35 ± 2°C for 48 h for MIC readings. The fractional inhibitory concentration index (FICI) was calculated as the sum of: FICA + FICB, where A represents A1Cl, B represents fluconazole. The FICA = (MICA combined)/(MICA alone), while the FICB = (MICB combined)/(MICB alone). The FICI was interpreted in the following way: synergism (<0.5), additivity (0.5–1.0), indifference (>1.0 and <4.0) or antagonism (>4.0; Lewis et al., 2002).

Effects on fungal micromorphology

The effects of A1Cl and fluconazole on morphological alterations of *C. tropicalis* and *C. parapsilosis* were evaluated using the slide culture technique. We used the solid corn meal agar medium with Tween 80 at 2% (CA; Hi Media Laboratories) (Alves et al., 2013). Aliquots of 100 μl of test drugs (MIC, 2 × MIC and 4 × MIC) were added to the culture medium. We also performed control tests without drugs. Recent fungal cultures were seeded onto the medium and covered with coverslips. The plates were incubated at 35 ± 2°C for 48 h in a moist chamber. Finally, the slides were examined under light microscopy (Nikon Eclipse Ci®) at 400×. We analysed five different fields of each slide, registering the production of yeast cells, pseudohyphae and chlamydoconidia. The scores of production intensity were high (+++), moderate (++), low (+) and absent (−).

In vitro biofilm susceptibility testing

We analysed the effects of different concentrations of A1Cl and fluconazole on biofilm formation, and mature biofilm sensitivity of *C. tropicalis* and *C. parapsilosis* strains on 96-well polystyrene plates. For the biofilm formation inhibition assay, 100 μl of RPMI-1640 containing the test drugs (1/4MIC, 1/2MIC, MIC, 2 × MIC, 4 × MIC) were added to wells. Then, 10 μl of inoculums was added, and the plates were incubated for a period of 48 h at 35 ± 2°C. Control was made without the drugs. After incubation, the contents of the wells were discarded, washed with 200 μl of distilled water and added 140 μl of 1% crystal violet solution (Newprov®). Plates were incubated for 40 min, without shaking. Finally, we removed the dye and added 140 μl of absolute ethanol (Rioquímica®). After 30 min, the plate was read in a microplate spectrophotometer (Multiskan GO) at 590 nm (Balasubramanian et al., 2012; Onsare & Arora, 2014). For drug sensitivity analysis of mature biofilm, 100 μl of RPMI-1640 medium were incubated with 10 μl of fungal inocula for 48 h at 35 ± 2°C without agitation to ensure the biofilm formation phase (Onsare & Arora, 2014; Rajasekharan et al., 2017). Then, we discarded the content of the wells and added 100 μl of RPMI-1640, with different concentrations of the test drugs (1/4MIC, 1/2MIC, MIC, 2 × MIC, 4 × MIC) and incubated 48 hours again at 35 ± 2°C, with no agitation. Then, the entire procedure was performed as described above.

Acquisition of biological material for ex vivo models

The ex vivo assays were performed on healthy human nails (no apparent infection). Healthy nail samples were collected from 20 adult volunteers (minimum age 18 years) of both genders. Previously, this study was approved by the Human Research Ethics Committee of the Health Sciences Center of the Federal University of Paraíba (João Pessoa, Brazil) under code 4.120.514. For nail fragments, removal of all dirt and debris was adopted to remove any surface contaminants that could influence the analytical tests. The nail fragments were cut into pieces of about 0.5 cm, treated with ethanol for 15 min, dried at 28°C and finally autoclaved (1 atm, 120°C, 15 min). They were then kept in sealed tubes at room temperature until further use.

Ex vivo biofilm susceptibility testing

Biofilms were formed on the inner surface of human nails fragments placed inside 96-well polystyrene plates. Aliquots of 100 μl of the inocula (1.5×10^6 CFU/ml) were transferred into each well containing nail fragments, and

plates were incubated for 90 min at 36°C (adhesion phase; Vila, Quintanilha, & Rozental, 2015). Cell suspensions were gently aspirated, and then 100-μl aliquots of RPMI 1640 medium (Sigma-Aldrich Co.) supplemented with 2% glucose and 20% foetal bovine serum (FBS; Gibco®) were added to each well to allow biofilm growth along the nail surface (Vila, Rozental, & De Sá Guimarães, 2015). Next, a 100-μl aliquot of A1Cl and fluconazole (1/4MIC, 1/2MIC, MIC, 2 × MIC, 4 × MIC) was added to the wells to analyse inhibition of biofilm formation. Plates were incubated at 35 ± 2°C/48 h. After incubation, we aspirate the wells and wash with 100 μl of sterile distilled water to release the biofilm formed on nails. A 10-μl aliquot of the supernatant was removed from each well, diluted (1100) and seeded on plates with Sabouraud dextrose agar. The plates were incubated at 35 ± 2°C/48 h to count the colony-forming units (CFU/mL). For drug sensitivity analysis of the mature biofilm, 100 μl of A1Cl and fluconazole (1/4MIC, 1/2MIC, MIC, 2 × MIC, 4 × MIC) were added to the wells with the formed biofilm, and incubated 48 h again at 35 ± 2°C, with no agitation. Then, the entire procedure was performed as described above by counting CFU/ml.

Molecular docking

Initially, the chemical structure of A1Cl was constructed in MarvinSketch (ChemAxon), and fluconazole structure was obtained from the PubChem chemical structure database (https://pubchem.ncbi.nlm.nih.gov). Then, they were grouped into a single SDF file created by the ChemAxon© Standardizer18.21.0 software (ChemAxon). This file contains the optimized structural data for molecular docking studies.

We selected cellular targets based on biological potential and structural arrangement, such as the slit width of the active site significantly greater than that of the human enzyme which provides the basis for designing potentially selective inhibitors (Marc et al., 1997). For this, we obtained 3D structures of the enzymes DHFR (Protein Data Bank ID: 1M79) and geranylgeranyltransferase-I (GGTase-I) (Protein Data Bank ID: 1MZC) crystallized from *Candida* species (https://www.rcsb.org/pdb/home/home.do) (Bernstein et al., 1977). The molecular targets (Protein Data Bank [PDB] format) and their binders were subjected to molecular docking using the Molegro Virtual Docker v.6.0.1 (MVD) software (Molexus) (Thomsen & Christensen, 2006).

The number of specific simulations is the number of times the coupling simulation is repeated for each binder. Sometimes more than one run is needed to identify good poses (particularly for binders with more than 15 flexible twists or if there are no promising cavities). A discrete grid with a resolution of 0.8 Å covering the protein was created

(Alves et al., 2020). We placed a sphere of radius 1.4 Å at each point of the grid and checked whether this sphere would overlap with any of the spheres determined by the Van der Waals radii of the protein atoms. The grid points where the probe collides with the spheres of the protein atoms were referred to as part of the inaccessible volume; all other points were referred to as accessible.

We used the MolDock SE (Simplex Evolution) algorithm with the following parameters: 10 runs with utmost 1500 interactions in 50 individuals, 2000 minimization steps for each flexible residue, and 2000 global minimization steps per run. Thus, the MolDock Score (GRID) was used to calculate the snap energy values (Thomsen & Christensen, 2006). A GRID was set at 0.3 Å, and the search sphere was set at 15 Å in radius. We evaluate internal electrostatic interactions and internal hydrogen bonds to verify the energy of the ligand.

Molecular dynamic

Redocking of the ligands complexed with the respective proteins was performed using root mean square deviation (RMSD) values which indicate the reliability of the modelling. In this analysis, smaller values are more favourable. This parameter is calculated based on the overlapping structures deviation of the binder complexed with the protein and the pose generated by this molecular coupling. We use the same modelling settings as described earlier.

Models were created using these ligands as a reference for proteins with ligands complexed with these structures.

Statistical analysis

The MIC and MFC values were expressed as a modal value of the results (triplicate). In vitro and ex vivo assays were performed in triplicate, and the results were expressed as mean ± standard deviation (SD). We submitted the data to the Kolmogorov–Smirnov test to analyse the normality and homoscedasticity of residuals, both at a significance level of 5% ($p > 0.05$). The results were submitted to one-way ANOVA, followed by Tukey's post-tests to determine the difference between groups. p-values lower than 0.05 were considered significant.

RESULTS

Fungal susceptibility

MIC values for A1Cl ranged from 16 to 256 μg/ml for all *C. tropicalis* and *C. parapsilosis* strains. Fluconazole

MIC values ranged from 16 to 512 µg/ml (Table 1). MFC values for all strains varied from 16 to 512 µg/ml (Table 1). In addition, fungal growth was detected when all strains were cultured in the absence of drugs (inoculum viability), whereas DMSO 5% at Tween 80 2% did not inhibit fungal growth. Based on these results, we confirm that A1Cl has a fungicidal effect under the conditions evaluated. Starting from this step, we selected three strains of each fungal species to be used in the subsequent assays: *C. tropicalis* ATCC-13803, LM-98 and LM-111; *C. parapsilosis* ATCC-22019, LM-78 and LM-197.

Study of association between drugs

Considering that the synthetic molecule A1Cl had shown a fungicidal effect against all yeasts, we proceeded to study the association between A1Cl and fluconazole. The combination between A1Cl and fluconazole did not decrease the MIC values compared to the respective MIC values alone. Thus, the combination of A1Cl and fluconazole showed indifferent antifungal effects (ICIF ≥ 1 and ≤ 4) (Table 2).

Effects on fungal micromorphology

The images representing the growth of fungal strains showed *Candida* virulence structures: pseudohyphae, blastoconidia and chlamydoconidia (Figures 1 and 2). In the absence of drugs, we observed the presence of pseudohyphae, blastoconidia and chlamydoconidia. However, the strains decreased the production of blastoconidia,

pseudohyphae and chlamydoconidia in the presence of A1Cl and fluconazole (Table 3). We concluded that A1Cl inhibited the production of virulence structures in a concentration-dependent way.

In vitro biofilm susceptibility testing

A1Cl inhibited biofilm formation in vitro at all concentrations tested (1/4MIC to 4 × MIC) against *C. tropicalis* and *C. parapsilosis* ($p < 0.05$). Sub-CIM inhibited 30% biofilm formation compared to the control. Inhibitory effects increased as drug concentrations increased. A1Cl showed similar results in the assay to assess the sensitivity of mature biofilm to drugs. In this case, the biofilm biomass of *C. tropicalis* and *C. parapsilosis* significantly decreased compared to the control ($p < 0.05$) as the drug concentration increased. A1Cl (at concentrations higher than MIC) inhibited more than 60% in vitro biofilm formation and reduced above 57% of mature biofilm compared to controls. In order for fluconazole to achieve the same antibiofilm effect by more than 50%, 4 × MIC was required (Figures 3–6). Finally, our results suggest that the antibiofilm effect of A1Cl occurs in a concentration-dependent manner.

Ex vivo biofilm susceptibility testing

Initially, the experimental conditions presented in this study induced the formation and viability of biofilm by the tested strains. A1Cl and fluconazole showed better results at MIC, 2 × CIM, 4 × MIC, concentrations (Figures 7–10). A1Cl (MIC) reduced more than 50% of the CFU of

TABLE 1 MIC and MFC values (µg ml^{-1})[a] of A1Cl and fluconazole against *Candida tropicalis* and *Candida parapsilosis* strains

	A1Cl			Fluconazole		
Fungi	MIC	MFC	MFC/MIC	MIC	MFC	MFC/MIC
Candida tropicalis						
ATCC-13803	16	16	Fungicide	16	16	Fungicide
LM-98	128	128	Fungicide	256	256	Fungicide
LM-111	256	256	Fungicide	256	256	Fungicide
LM-135	256	256	Fungicide	512	512	Fungicide
Candida parapsilosis						
ATCC-22019	16	16	Fungicide	16	16	Fungicide
LM-78	256	128	Fungicide	256	256	Fungicide
LM-197	256	512	Fungicide	512	512	Fungicide
LM-707	256	512	Fungicide	512	512	Fungicide

Abbreviations: MIC, minimal inhibitory concentration; MFC, minimal fungicide concentration.

[a]Model values of three experiments.

the biofilm formed by the fungal strains ($p < 0.05$). The drugs also decreased the viability of the mature biofilm ($p < 0.05$). Thus, we show the potent antibiofilm effect in ex vivo models of human nail fragments, corroborating the in vitro results.

TABLE 2 Association study of A1Cl and fluconazole against *Candida tropicalis* and *Candida parapsilosis* strains

Fungi	FIC alone	FIC combined	FICI index (type of interaction)
Candida tropicalis			
ATCC-13803	1	1	2 (indifferent)
LM-98	1	1	2 (indifferent)
LM-111	1	2	3 (indifferent)
Candida parapsilosis			
ATCC-22019	1	1	2 (indifferent)
LM-78	0.5	2	2.5 (indifferent)
LM-197	1	0.5	1.5 (indifferent)

Abbreviations: MIC, minimum inhibitory concentration ($\mu g\ ml^{-1}$); FIC, fractional inhibitory concentration.

Molecular docking

Initially, A1Cl was subjected to molecular coupling with DHFR and GGTase-I to investigate possible binding at active sites. The analysis of docking prediction results was based on the Moldockscore and Rerankscore scoring functions, where more negative values indicated better docking predictions. We observed that the DHFR crystallographic ligand had RMSD 0.19 Å, and the ligand complexed to GGTase-I had RMSD 0.19 Å during the redocking analysis. In this context, we consider the values satisfactory and the docking reliable.

A1Cl presented binding energy values higher or close to fluconazole in at least one scoring function, concluding that it interferes with the functionality of the evaluated targets (Table 4). Considering that A1Cl had lower binding energy than the PDB ligand for DHFR, we argue that this enzyme is a susceptible target to the action of A1Cl. Furthermore, A1Cl was able to form a hydrogen bond with the amino acid Glu32, van der Waals interaction with the amino acid Val10, electrostatic interaction with the amino acid Met25 and hydrophobic interaction with the amino acid Phe36 at the active site of the enzyme DHFR (Figure 11).
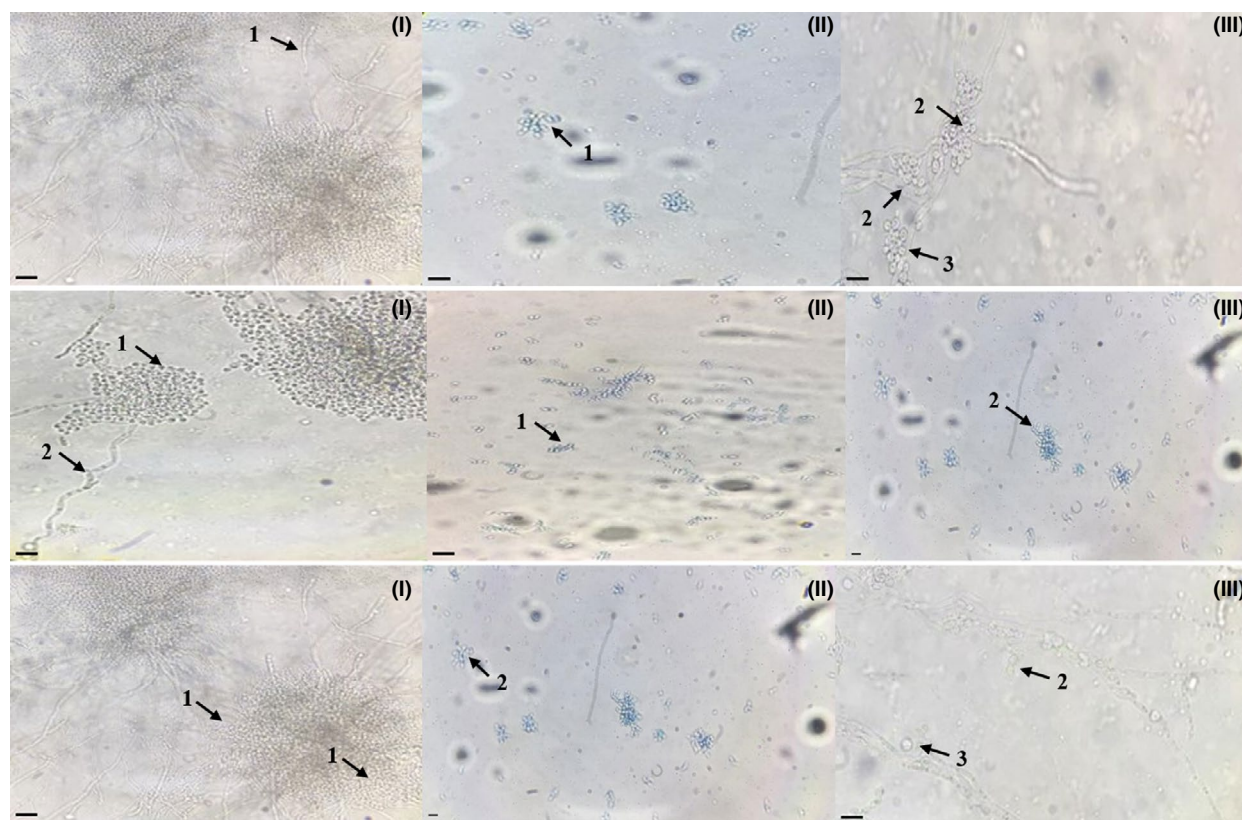
FIGURE 1 Analysis of the morphology of *Candida tropicalis* (a) ATTC-13803, (b) LM-98, and (c) LM-111 by optical microscopy in the absence of drugs (I), A1Cl (II), and fluconazole (III). Magnification 400, scale 100 µm. The images show individual yeasts cells (1), pseudohyphae (2) and chlamydoconidia (3)
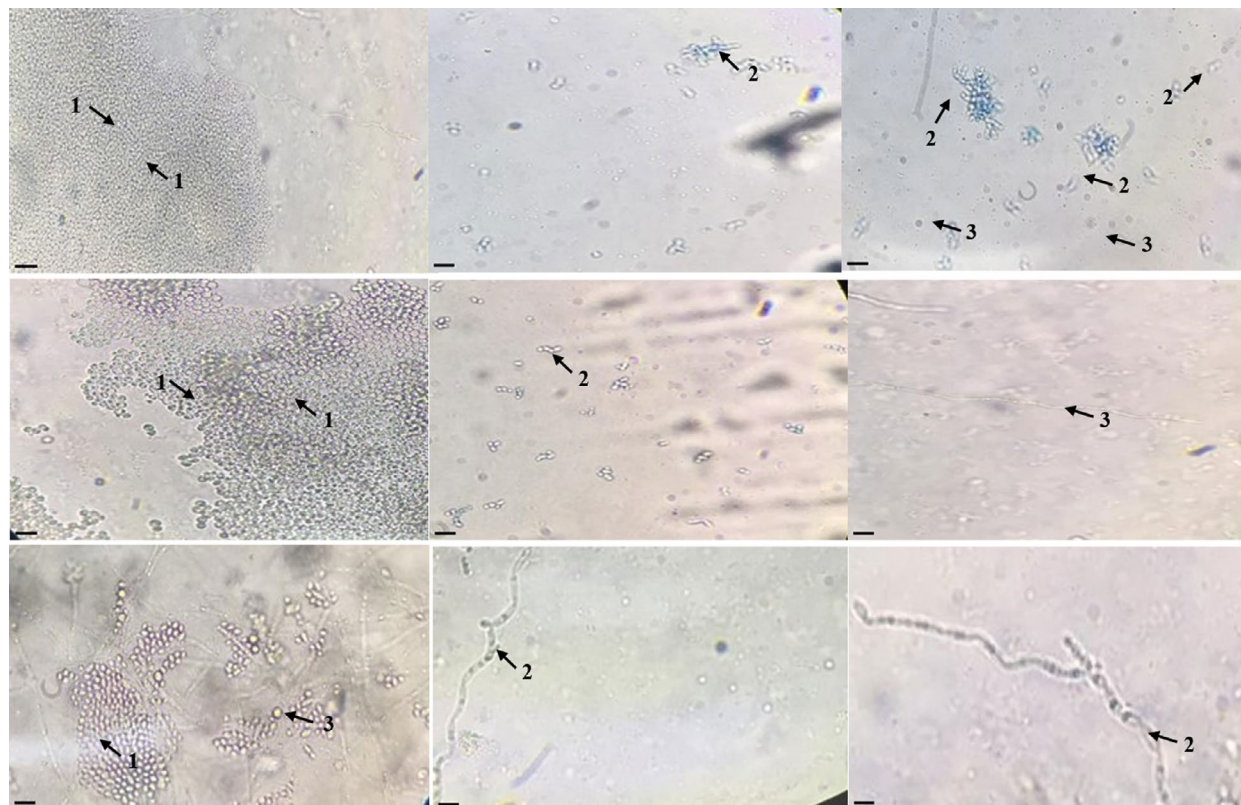
FIGURE 2 Analysis of the morphology of *Candida parapsilosis* (a) ATTC-22019, (b) LM-78, and (c) LM-197 by optical microscopy in the absence of drugs (I), A1Cl (II), and fluconazole (III). Magnification 400, scale 100 μm. The images show individual yeasts cells (1), pseudohyphae (2) and chlamydoconidia (3)

TABLE 3 Morphological alterations of *Candida tropicalis* and *C. parapsilosis* in the absence (control) and presence of A1Cl and fluconazole

Drugs (μg ml^{-1})	*C. tropicalis*			*C. parapsilosis*		
	ATCC-13803	LM-98	LM-111	ATCC-22019	LM-78	LM-197
A1Cl						
MIC	++	+++	++	++	++	++
2 × MIC	++	++	+	++	++	++
4 × MIC	++	+	+	+	+	++
Fluconazole						
MIC	+++	+++	+++	+++	+++	+++
2 × MIC	++	+++	++	+++	+++	+++
4 × MIC	++	++	++	++	+	+

Note ≥ +++ High recurrence of hyphae, pseudohyphae, blastoconidia and chlamydoconidia.≤ ++ Moderate recurrence of hyphae, pseudohyphae and chlamydoconidia.≤ − Absence of hyphae, blastoconidia and absence of pseudohyphae.

Molecular dynamic

We performed molecular dynamics simulations to investigate whether A1Cl and fluconazole can bind to proteins under the influence of the environment (solvent and proteic conformational changes). For this, RMSD was calculated for the Cα atoms of A1Cl. The A1Cl RMSD showed stability during the dynamic phase with variations between 5 and 8 ns, revealing more excellent stability than the PDB ligand. Furthermore, A1Cl remained stable within the DHFR active site, even under the influence of solvents and molecular flexibilizations (Figure 12). To understand the different conformational changes of DHFR, we calculated the root mean square fluctuation (RMSF) for each amino acid. Considering that fluctuations above 0.3 nm contribute to protein flexibility, we found that among the
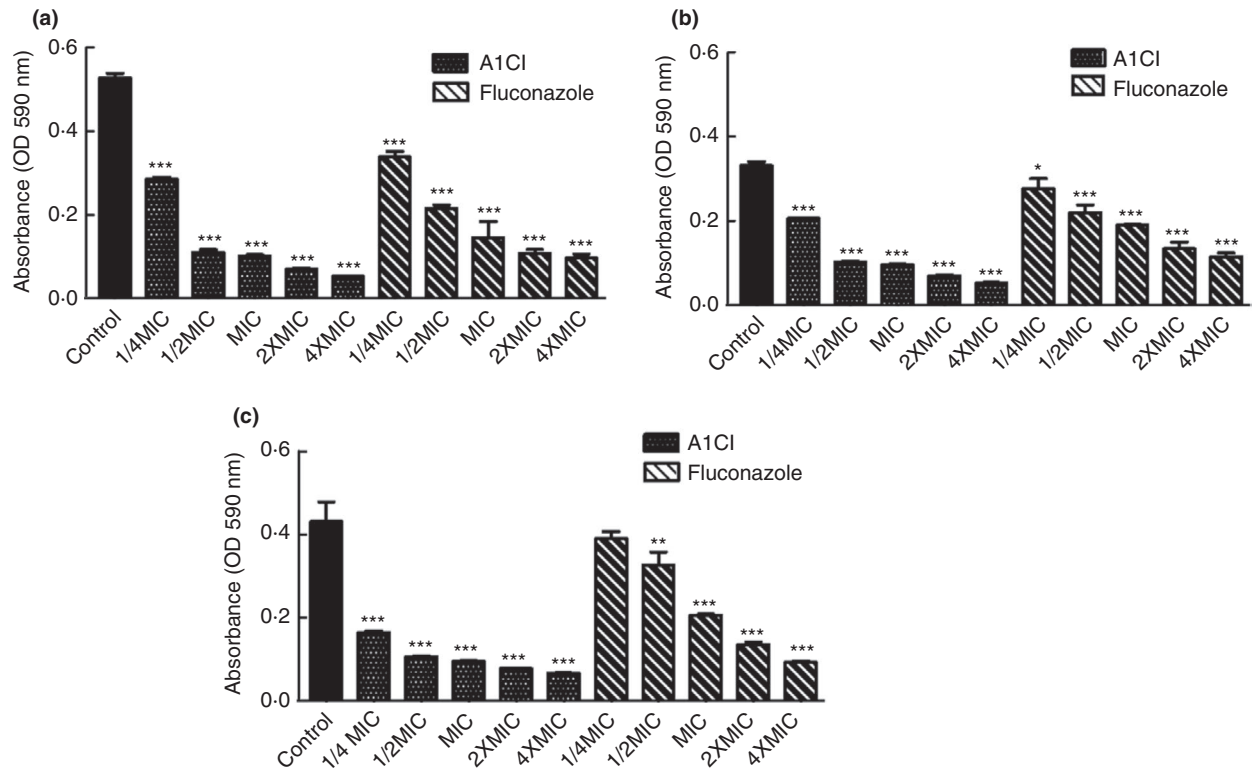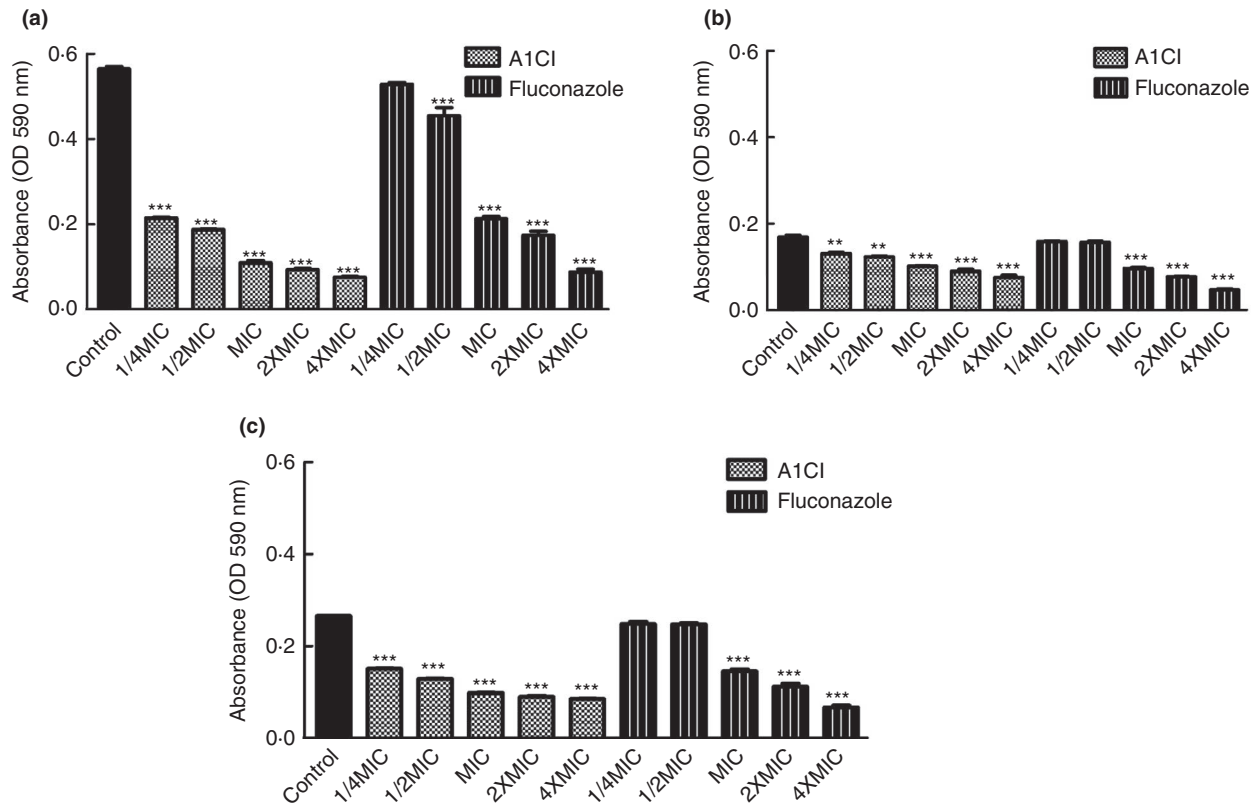
FIGURE 3 Inhibitory effect of A1Cl and fluconazole on the in vitro biofilm formation of *Candida tropicalis* (a) ATCC-13803, (b) LM-98, and (c) LM-111. Results are expressed as arithmetic mean. One-way ANOVA: followed by Tukey's post-test. Statistical analysis compared to control: *$p \leq 0.05$, **$p \leq 0.01$, ***$p \leq 0.001$
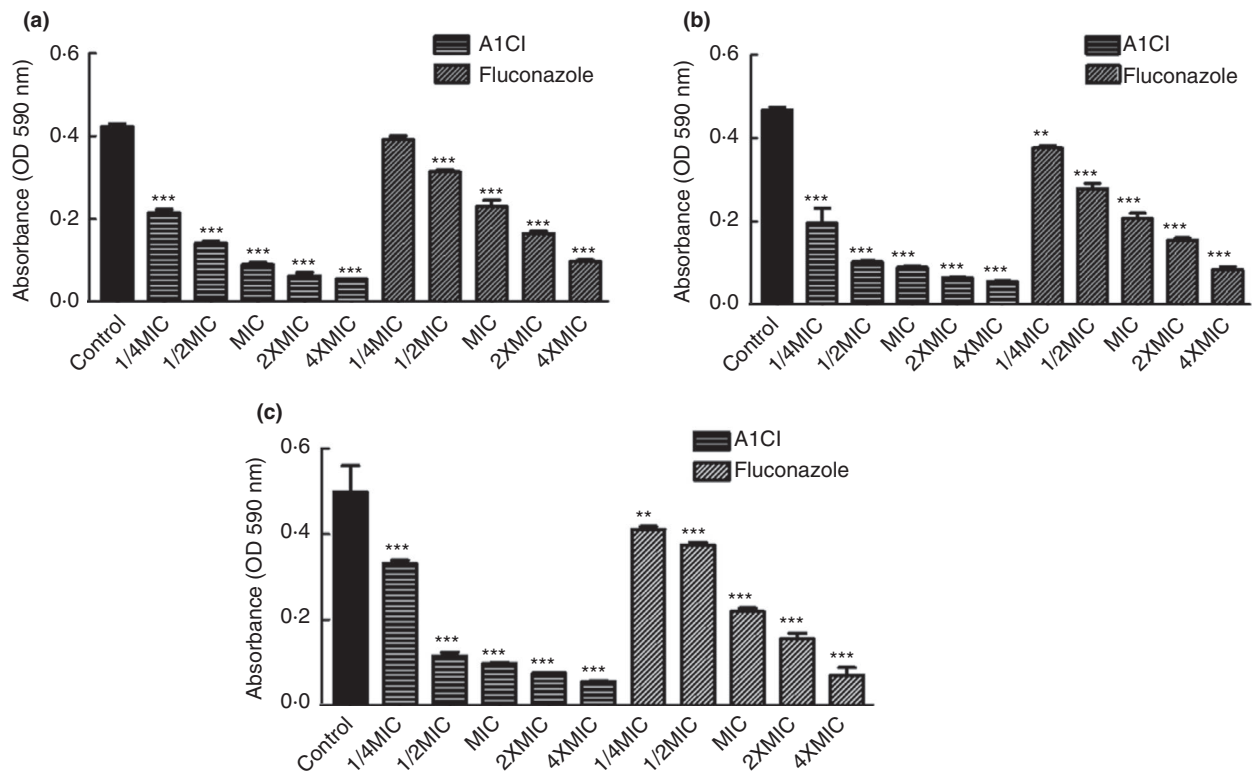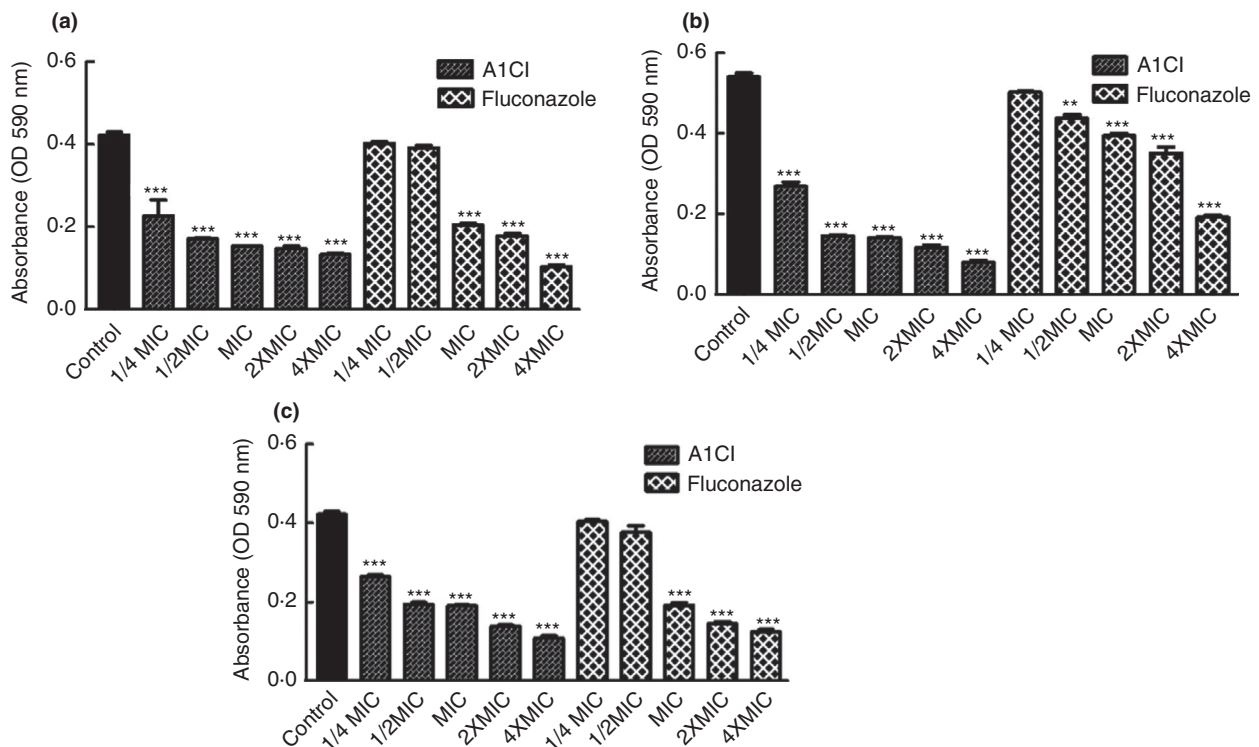

FIGURE 4 Inhibitory effect of A1Cl and fluconazole on the in vitro biofilm formation of *Candida parapsilosis* (a) ATCC-22019, (b) LM-78, and (c) LM-178. Results are expressed as arithmetic mean. One-way ANOVA: followed by Tukey's post-test. Statistical analysis compared to control: **$p \leq 0.01$, ***$p \leq 0.001$
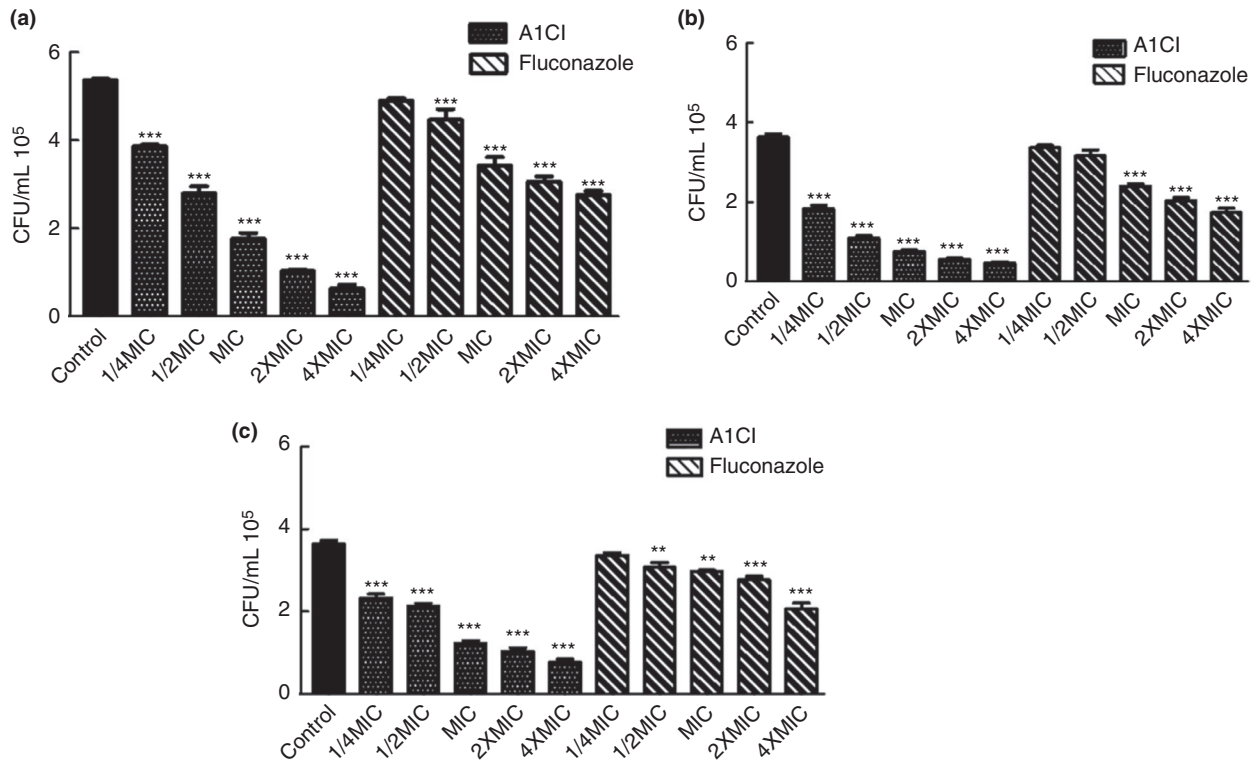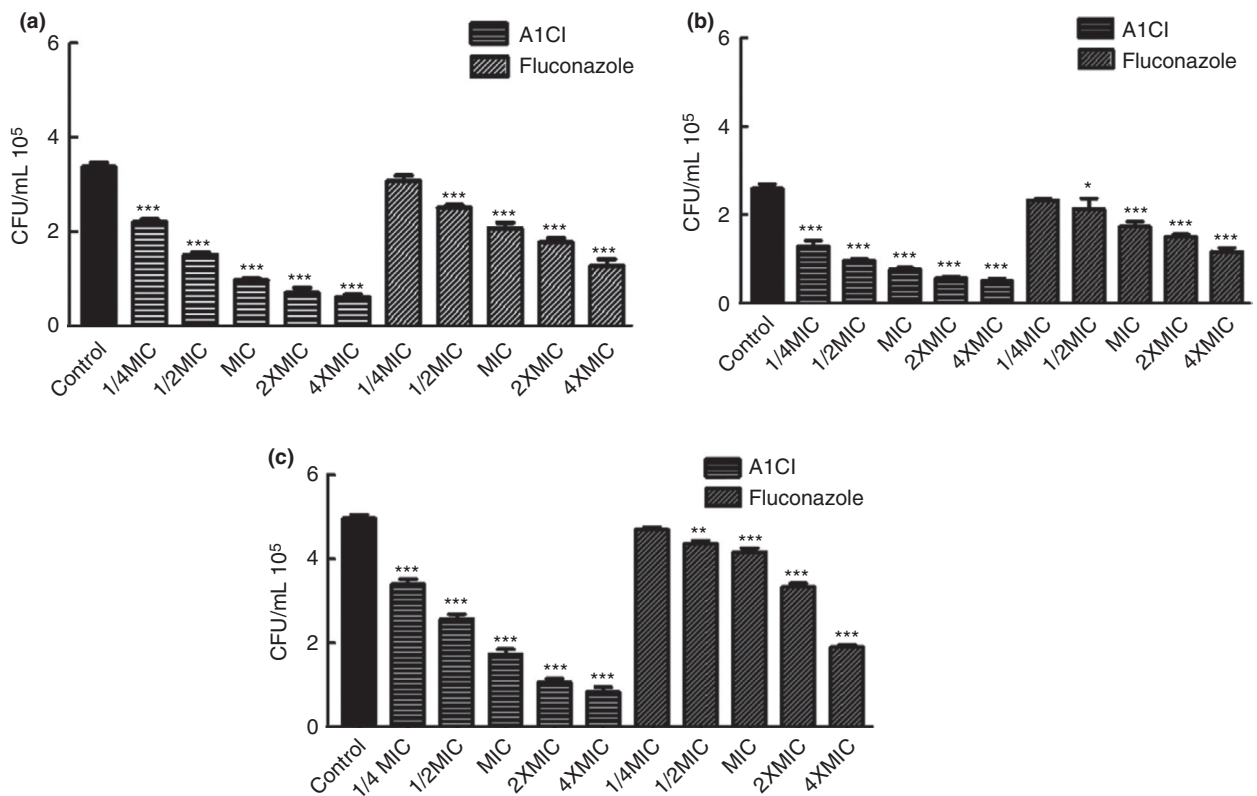
FIGURE 5 Inhibitory effect of A1Cl and fluconazole on in vitro biofilm biomass disruption of *Candida tropicalis* (a) ATCC-13803, (b) LM-98, and (c) LM-111. Results are expressed as arithmetic mean. One-way ANOVA: followed by Tukey's post-test. Statistical analysis compared to control: $**p \leq 0.01$, $***p \leq 0.001$
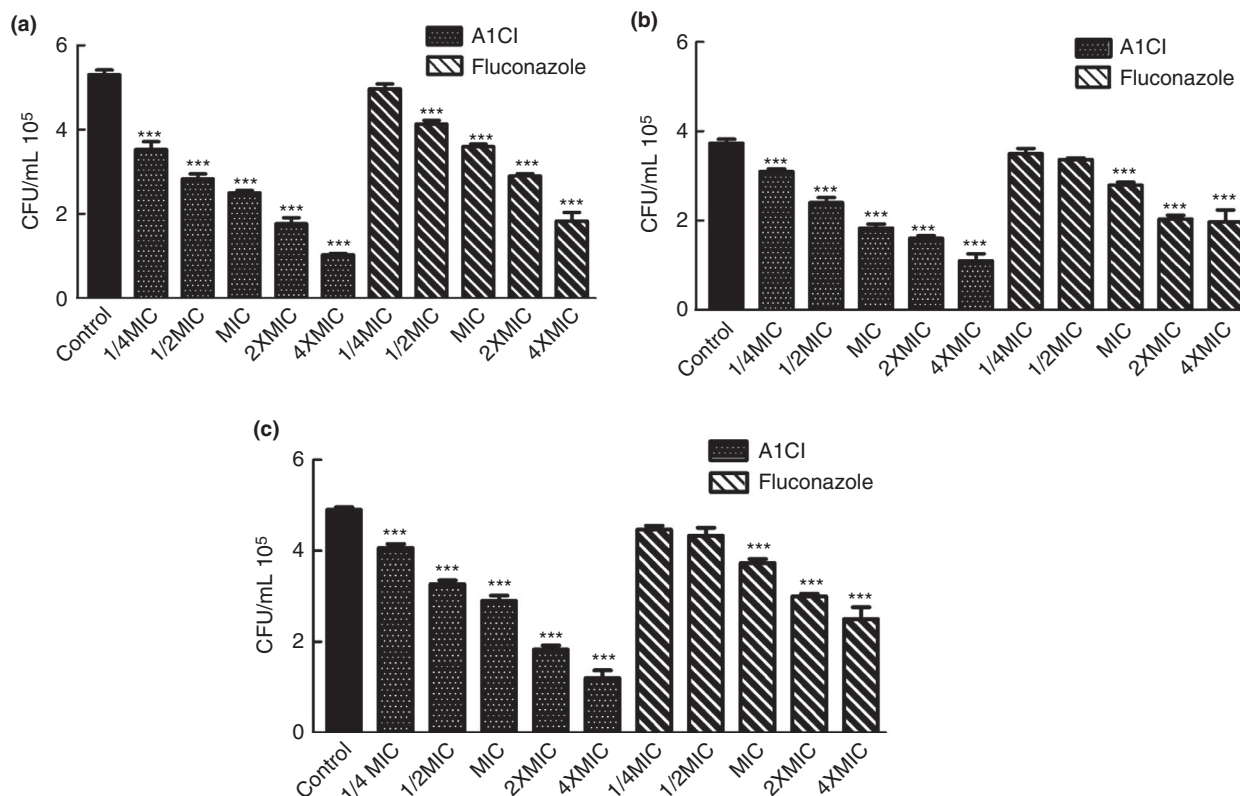

FIGURE 6 Inhibitory effect of A1Cl and fluconazole on in vitro biofilm biomass disruption of *Candida parapsilosis* (a) ATCC-13803, (b) LM-78, and (c) LM-197. Results are expressed as arithmetic mean. One-way ANOVA: followed by Tukey's post-test. Statistical analysis compared to control: $**p \leq 0.01$, $***p \leq 0.001$

FIGURE 7 Antibiofilm effect of A1Cl and fluconazole on nail fragments (*ex vivo*) of *Candida tropicalis* (a) ATTC-13803, (b) LM-98, and (c) LM-111. One-way ANOVA: followed by Tukey's post-test. Statistical analysis compared to control: $**p \leq 0.01$, $***p \leq 0.001$

FIGURE 8 Antibiofilm effect of A1Cl and fluconazole on nail fragments (ex vivo) of *Candida parapsilosis* (a) ATCC-22019, (b) LM-98, and (c) LM-111. One-way ANOVA: followed by Tukey's post-test. Statistical analysis compared to control: $*p \leq 0.05$, $**p \leq 0.01$, $***p \leq 0.001$

FIGURE 9 Antibiofilm effect of A1Cl and fluconazole on rupture of preformed biofilms in nail fragments (ex vivo) against *Candida tropicalis* (a) ATCC-13803, (b) LM-98, and (c) LM-111. One-way ANOVA: followed by Tukey's post-test. Statistical analysis compared to control: **$p \leq 0.01$, ***$p \leq 0.001$

192 amino acid residues, only those at 1, 2 and 65 were responsible for the conformational changes (Figure 13). Finally, they did not influence the affinity and energy of A1Cl binding to the active site of the protein (Figure 14).

DISCUSSION

The treatment of onychomycosis remains a relevant public health problem. Current drug treatments are effective, but resistant and biofilm-forming strains are emerging, causing therapeutic failures (Silva et al., 2017). Therefore, the need to search for new antifungal drugs against onychomycosis agents persists. In this sense, optimizing the synthesis processes, obtaining and purification of molecules associated with in vivo and in silico biological studies have excellent potential to improve therapeutic efficacy and reduce the cost of acquiring new antifungal molecules (Blakemore et al., 2018).

There is evidence that the insertion of chlorine atoms potentiates antifungal effects of synthetic molecules (Liu et al., 2019). In the acetamide group, the presence of the chlorine atom improves antimicrobial activity. Furthermore, antifungal activity of N-(2-hydroxyphenyl) acetamide against *C. albicans* was evaluated, and they

observed that the same drug with a chlorine atom to the alpha carbon (2-chloro-N-(2-hydroxyphenyl) acetamide) was able to inhibit 96.6% of the growth of only one strain of *C. albicans* (Bravo et al., 2003).

We investigated the antifungal, antibiofilm and molecular predictions of A1Cl against clinical isolates of *C. tropicalis* and *C. parapsilosis*. We confirmed the fungicidal activity of A1Cl against all fungal strains used in this study. Our results demonstrate that A1Cl potential was higher than fluconazole, an oral azole drug to treat onychomycosis (Gupta et al., 2020). Similar results were achieved by Soyer and Eraç (2007), in which the introduction of chlorine atoms in the para position of the N-phenyl ring of acetamide derivatives potentiated the antimicrobial activity against clinical isolates of *S. aureus*.

In recent decades, *Candida* species has presented high resistance to fluconazole. This phenomenon can be explained, in part, as a result of selective pressure caused by prophylaxis, therapeutic management and irrational use of antifungals (Alves et al., 2020). For this reason, we evaluated possible interactions between A1Cl and fluconazole by checkerboard. This methodology is employed as a viable approach to assessing drug interactions to overcome the limitations of antifungal monotherapy (Silva et al., 2020). However, none of the associations positively modulated the antifungal action against
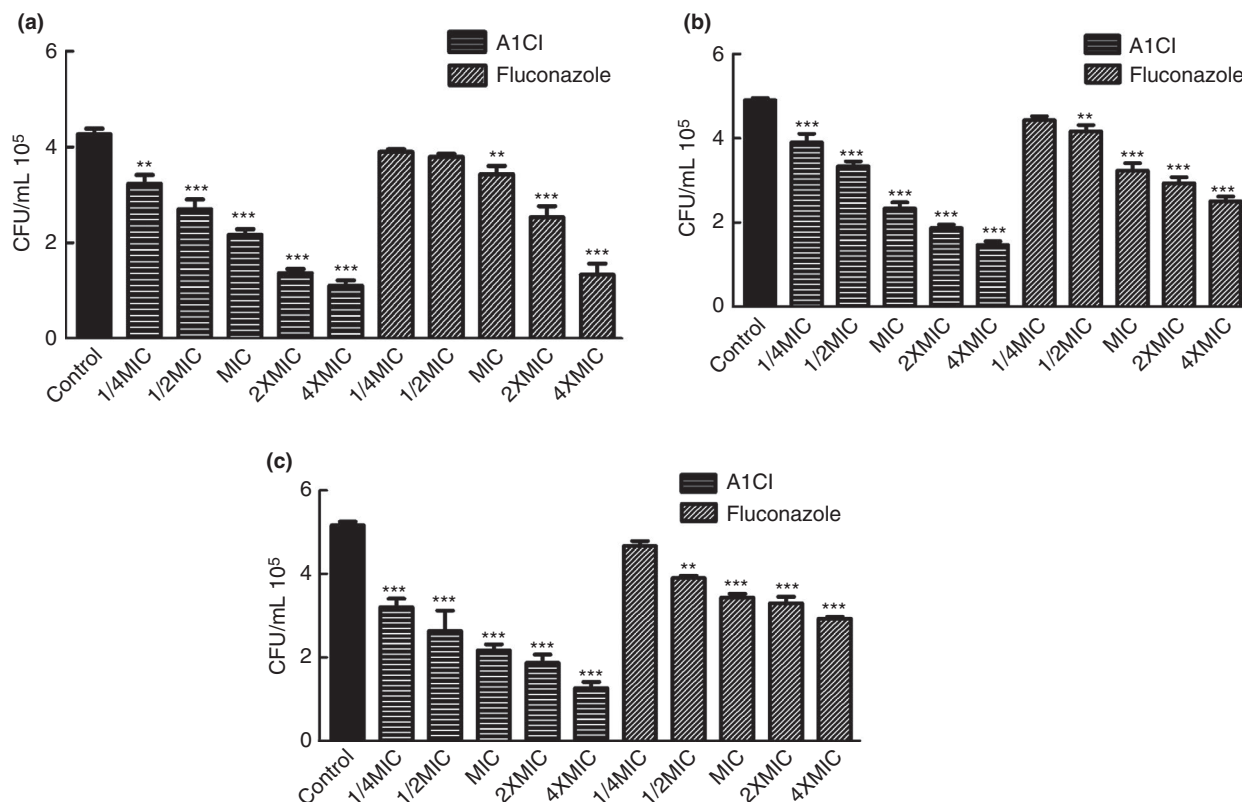
FIGURE 10 Antibiofilm effect of A1Cl and fluconazole on rupture of preformed biofilms in nail fragments (ex vivo) against *Candida parapsilosis* (a) ATCC-13803, (b) LM-78, and (c) LM-197. One-way ANOVA: followed by Tukey's post-test. Statistical analysis compared to control: **$p \leq 0.01$, ***$p \leq 0.001$

TABLE 4 Binding energies (Moldock and Rerank score) of PDB enzymes and tested compounds

	A1Cl		Fluconazole		PDB (Ligand)	
Enzyme	Moldock	Rerank	Moldock	Rerank	Moldock	Rerank
DHFR	−76.04	−65.30	−131.78	−106.20	−41.74	−38.45
GGTase-I	−55.48	−47.43	−66.01	−26.93	−158.16	−126.98

the fungal strains under experimental conditions (Table 3). Therefore, we continue our studies using A1Cl alone.

In the next step, we sought to observe which possible morphological changes the test drugs induce in strains of *C. tropicalis* and *C. parapsilosis*. The main fungal structures observed in our study were pseudohyphae, chlamydoconidia and blastoconidia. They are closely related to virulence because they participate in the adhesion and invasion of host tissues (Gago et al., 2014; Silva et al., 2011). In this context, the interference of A1Cl on the fungal morphology by A1Cl highlights its potent antivirulence effects.

Based on this premise, we evaluated a specific characteristic of the pathogenicity and virulence of *Candida* species: the ability to form biofilms. Biofilms protect fungi from external factors and contribute to the severity of the infection and resistance to antifungal drugs (Cavalheiro & Teixeira, 2018). Fungal biofilms are responsible for a broad spectrum of microbial infections in the human host (Barros et al., 2020). Therefore, effective pharmacological approaches against fungal biofilms promise to treat onychomycosis.

We observed that A1Cl showed antibiofilm potential against *C. tropicalis* and *C. parapsilosis* in vitro and ex vivo models in a concentration-dependent manner. This activity occurred in the early stages of fungal biofilm formation, as well as on mature biofilms. Our results agree with Kwasny and Opperman (2010), who classified a drug with good antibiofilm activity whether it inhibits ≥80% of biofilm growth and inhibits ≥40% of planktonic growth compared to controls. Fluconazole, in turn, needed concentrations greater than 4 × MIC to obtain activity similar

FIGURE 11 Interactions between A1Cl and the PDB ligand with active site of dihydrofolatereductase
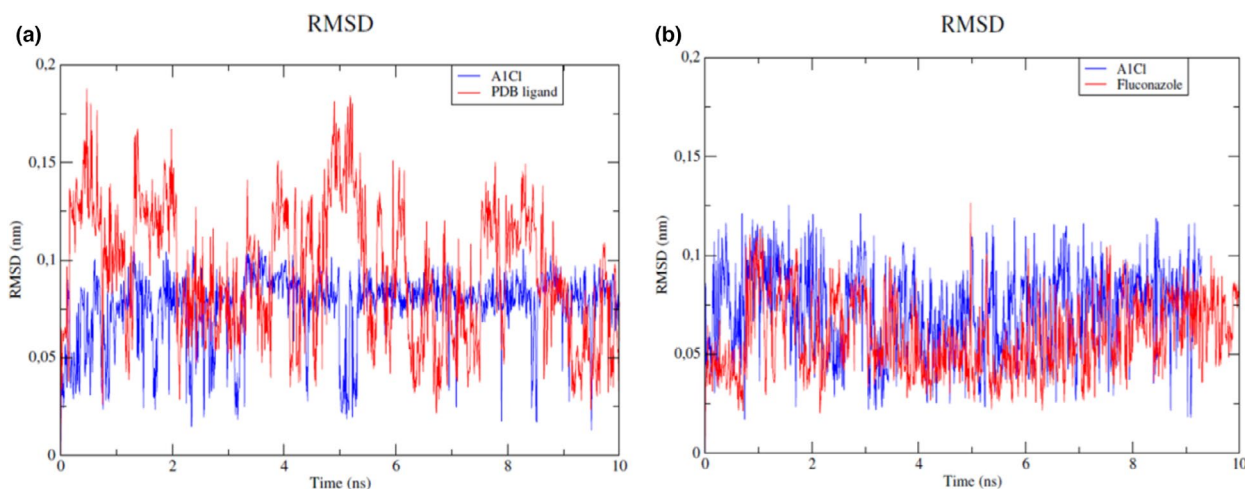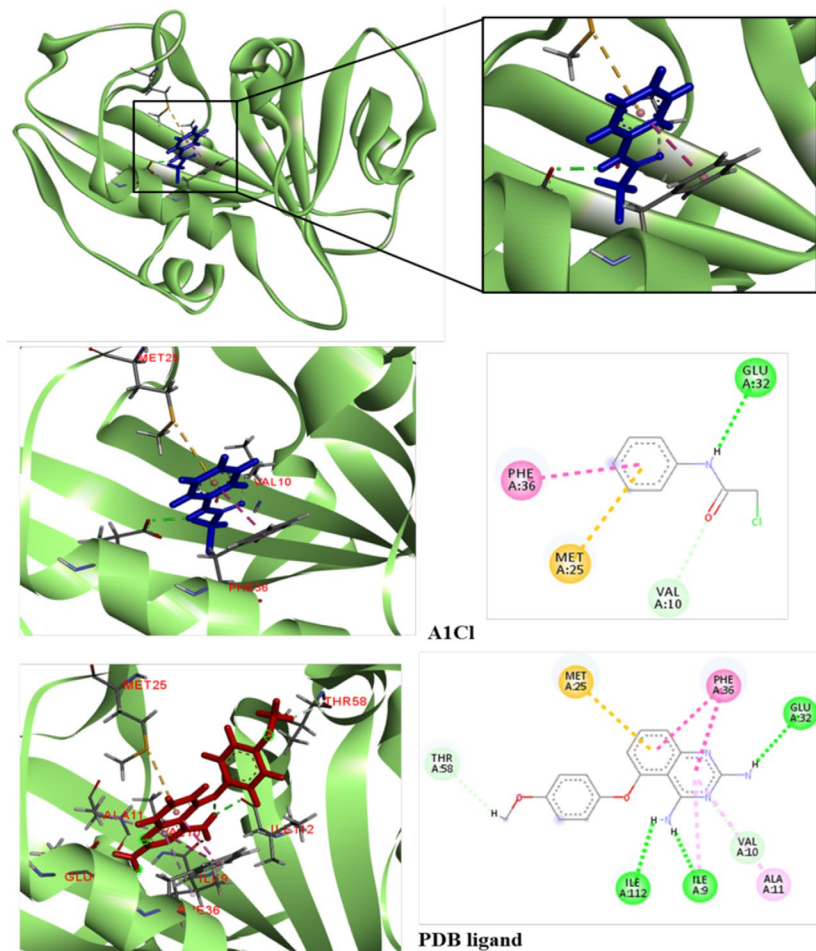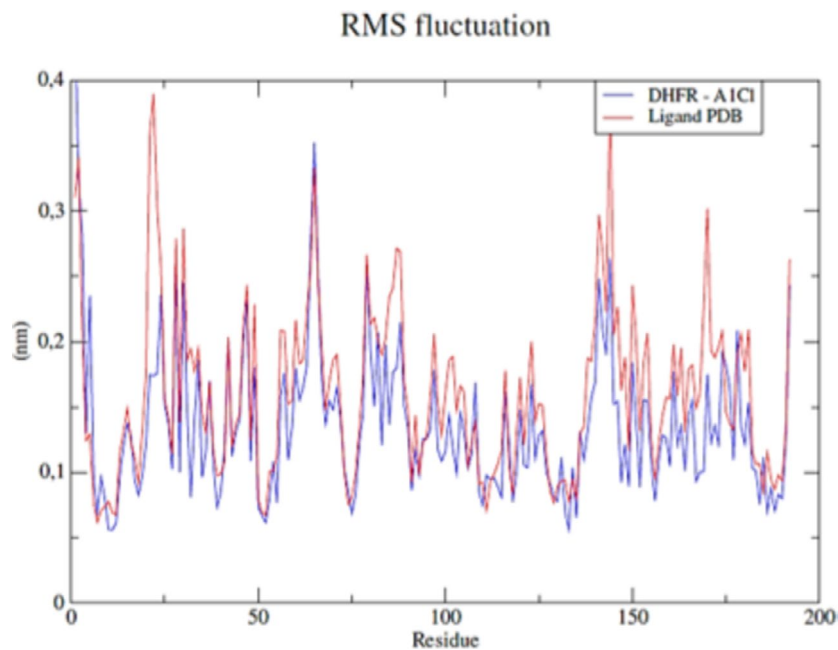

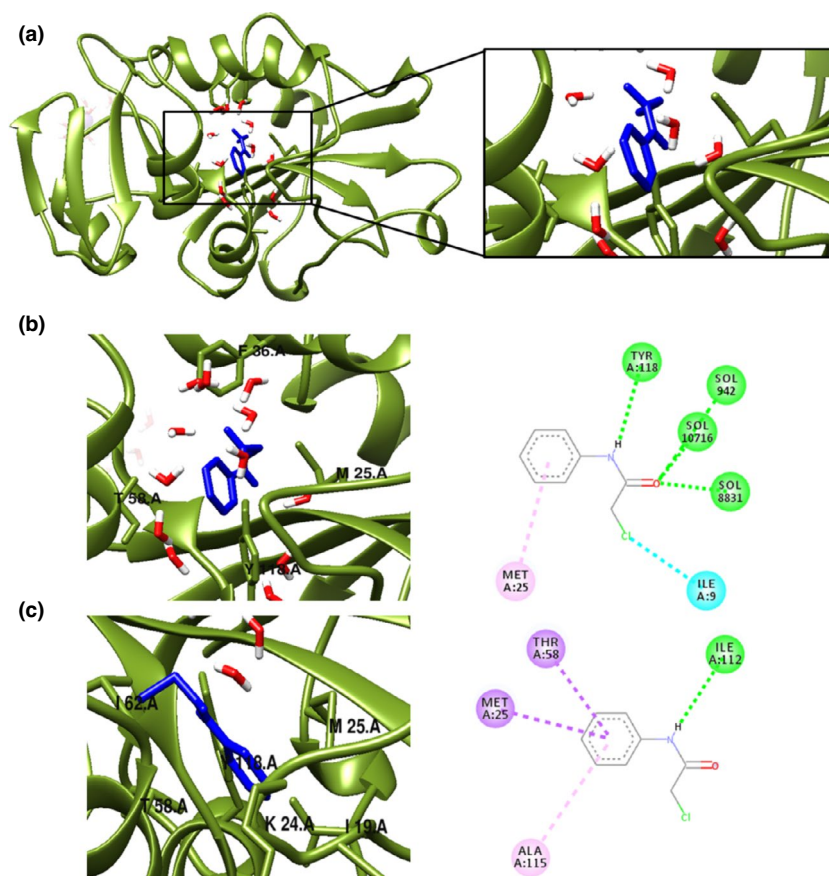**FIGURE 12** Root mean square deviation of A1Cl-PDB ligand (a), and A1Cl-fluconazole (b)

to A1Cl. El-Houssaini et al. (2019) showed that fluconazole has no antibiofilm effect at subinhibitory concentrations. Our results on ex vivo models were promising as it mimics human nail infections as much as possible. Gupta et al. (2019) described the low susceptibility of *Candida* species to fluconazole and that the drug did not inhibit biofilm development. Paškevičius et al. (2020) also showed resistance of *C. parapsilosis* and *C. tropicalis* biofilms to fluconazole.

Typically, drugs are more potent against planktonic cells than biofilms. In a biofilm lifestyle, fungi increase communication and virulence, enhance metabolic

cooperation and improve the regulation of gene expression (Lohse et al., 2020). In addition, the extracellular matrix also limits the effectiveness of antifungal drugs because it physically inhibits the contact of the drug with the micro-organism (Gupta, Mays, et al., 2018). The formation of extracellular material adhering to the nail plates favours progression to onychomycosis, which may explain resistance to antifungal treatment and disease recurrence (Vila, Quintanilha, & Rozental, 2015).

Data referring to molecular targets are crucial for studies that analyse the potential of new drugs. Thus,

we performed in silico assays to predict the possible target cells involved in A1Cl antifungal activity. Among the in silico tools, the prediction of molecular docking stands out for the prospecting of protein targets in micro-organisms and ligands with high affinity (Silva et al., 2019). Furthermore, molecular docking studies help identify new compounds of therapeutic interest, predicting ligand–target interactions at a molecular level (Pinzi & Rastelli, 2019). In this study, we used two targets: DHFR and GGTase-I.

Our results showed that A1Cl damaged the fungal morphology, a fungal process that depends on cell wall integrity. GGTase-I is a heterodimeric zinc enzyme that plays a critical role in fungal cell wall integrity and morphogenesis. Furthermore, it has low amino acid similarity (30%) with the human isoform (Sun et al., 2020). Then, we explored the role of GGTase-I in the antifungal activity of A1Cl. However, based on molecular prediction results, the inhibition of this enzyme is not involved in the mechanism of action of A1Cl against *C. tropicalis* and *C. parapsilosis* (Table 4).

In contrast, A1Cl showed an affinity with DHFR and binding energy values higher than PBD ligand. DHFR enzyme as a therapeutic target in treating infections has been demonstrated since the middle of the last century. DHFR catalyses the reduction of dihydrofolate to tetrahydrofolate; thereby, it is involved in the synthesis of cell proliferation (Sanad et al., 2021). The inhibition of DHFR forms the basis for the treatment of many infectious diseases because it generates raw materials for DNA replication (Sanad et al., 2021). According to Whitlow et al. (1997), DHFR inhibitors interact with amino acids Ile8, Ile9, Val10, Ala11, Glu32 and Phe36, confirming the viability of inhibiting our compound with the target site (Figure 11).

Finally, we performed RMSD to evaluate the residue dynamics and the degree of flexibility by the ligand complexed to the active site of CaDHFR in the presence of the solvent. RMSD is essential in determining how drug binding to the active site of the target protein affects its ability to reach an equilibrium state and quantify the structural flexibility of protein–drug complexes during simulation (Joshi et al., 2021). In our results, the RMSD of the CaDHFR-A1Cl complex revealed stability around 2–3 ns and maintained its stability above 10 ns, suggesting better binding stability than the ligand (Figure 12). In this way, MD trajectories are globally stable during the simulation time for A1Cl.

RMSF is used to analyse how drug binding affects protein structural flexibility during DM simulation. The higher RMSF value indicates greater flexibility of the protein–ligand complex (Figure 13). We observed that the DHFR enzyme complexed to the compound A1Cl showed

interactions similar to those surveyed in docking after dynamic simulations at times of 200 and 600 ps. A1Cl remained in the active site even under the influence of solvents and structural flexibility. The RMSF was less than 0.3 nm, which means they were stable during the simulation MD. Then, A1Cl has the potential to inhibit the enzymatic activity of CaDHFR.

CONCLUSION

The discovery of new antifungal drugs against resistant agents is urgently needed, especially as therapeutic alternatives for onychomycosis. Therefore, our results are unprecedented and relevant to help overcome this scenario. In this sense, we present a new synthetic derivative with antibiofilm activity from *C. tropicalis* and *C. parapsilosis* in vitro and ex vivo models. Furthermore, in silico studies suggest that its activity involves the inhibition of the enzyme DHFR. Moreover, we recommend that this bioactive compound be used in preclinical and clinical toxicity studies to ensure the efficacy and safety of a new antifungal agent for onychomycosis caused by *Candida*.

CONFLICT OF INTEREST
No conflict of interest was declared.

DATA AVAILABILITY STATEMENT
The data that support the findings of this study are available from the corresponding author upon reasonable request.

ORCID
Shellygton Lima Silva https://orcid.org/0000-0001-7168-7725
Luciana Scotti https://orcid.org/0000-0003-1866-4107

REFERENCES
Alves D. N., Monteiro, A. F. M., Andrade, P. N., Lazarini, J. G., Abílio, G. M. F., Guerra, F. Q. S., Scotti, M. T., Scotti, L., Rosalen, P. L. And Castro, R. D. D. (2020) Docking prediction, antifungal activity, anti-biofilm effects on *Candida* spp., and toxicity against human cells of cinnamaldehyde. *Molecules* 25(24), 5969.

Alves, L.A., Freires, I.D.A., Pereira, T.M., Souza, A.D., Lima, E.D.O. & Castro, R.D. (2013) Effect of *Schinus terebinthifolius* on *Candida albicans* growth kinetics, cell wall formation and micromorphology. *Acta Odontologica Scandinavica*, 71(3–4), 965–971.

Andrés, T.S. & Alexandro, B. (2020) *Candida* onychomycosis: an old problem in modern times. *Current Fungal Infection Reports*, 14(3), 206–216.

Arrua, J.M.M., Rodrigues, L.A.S., Pereira, F.O. & Lima, E.O. (2015) Prevalence of *Candida tropicalis* and *Candida krusei* in onychomycosis in João Pessoa, Paraiba, Brazil from 1999 to 2010. *Proceedings of the Brazilian Academy of Sciences*, 87(3), 1819–1822.

Balasubramanian, D., Schneper, L., Merighi, M., Smith, R., Narasimhan, G., Lory, S. et al. (2012) The regulatory repertoire of *Pseudomonas aeruginosa* AmpC ß-lactamase regulator AmpR includes virulence genes. *PLoS ONE*, 7(3), 34067.

Barros, P.P., Rossoni, R.D., De Souza, C.M., Scorzoni, L., Fenley, J.D.C. & Junqueira, J.C. (2020) *Candida* biofilms: an update on developmental mechanisms and therapeutic challenges. *Mycopathologia*, 185(3), 415–424.

Bernstein, F.C., Koetzle, T.F., Williams, G.J., Meyer, E.F., Jr., Brice, M.D., Rodgers, J.R. et al. (1977) The Protein Data Bank: a computer-based archival file for macromolecular structures. *Journal of Molecular Biology*, 112(3), 535–542.

Blakemore, D.C., Castro, L., Churcher, I., Rees, D.C., Thomas, A.W., Wilson, D.M. et al. (2018) Organic synthesis provides opportunities to transform drug discovery. *Nature Chemistry*, 10(4), 383–394.

Bravo, H.R., Weiss-López, B., Lamborot, M. & Copaja, S. (2003) Chemical basis for theantimicrobialactivityofacetanilides. *Journal of the Chilean Chemical Society*, 48, 27–30.

Cavalheiro, M. & Teixeira, M. C. (2018) *Candida biofilms*: threats, challenges, and promising strategies. *Frontiers in Medicine* 5, 28.

Clinical and Laboratory Standards Institute. (2017) *Reference method for broth dilution antifungal susceptibility testing of yeasts. Approved standard, 4th edition. CLSI document M27-A4.* Wayne, PA: Clinical and Laboratory Standards Institute.

Cordeiro, L.V., Neto, H.D., Figueiredo, P., Souza, H., Sousa, A., Andrade-Júnior, F. et al. (2020) Potential of 2-chloro-*N*-(4-fluoro-3-nitrophenyl) acetamide against *Klebsiella pneumoniae* and *in vitro* toxicity analysis. *Molecules*, 25(17), 3959.

El-Houssaini, H.H., Elnabawy, O.M., Nasser, H.A. & Elkhatib, W.F. (2019) Influence of subinhibitory antifungal concentrations on extracellular hydrolases and biofilm production by *Candida albicans* recovered from Egyptian patients. *BMC Infectious Diseases*, 19(1), 1–9.

Ferreira, E.S., Cordeiro, L.V., Silva, D.F., Souza, H.D.S., Athayde-Filho, P.F., Barbosa-Filho, J.M. et al. (2021) Antifungal activity and mechanism of action of 2-chloro-N-phenylacetamide: a new molecule with activity against strains of *Aspergillus flavus*. *Anais da Academia Brasileira de Ciências*, 93(3), 1–15.

Gago, S., García-Rodas, R., Cuesta, I., Mellado, E. & Alastruey-Izquierdo, A. (2014) *Candida parapsilosis, Candida orthopsilosis and Candida metapsilosis* virulence in the non-conventional host *Galleria mellonella*. *Virulence*, 5(2), 278–285.

Gupta, A.K., Jessie, C. & Neil, H.S. (2018) Antibiofilm treatment for onychomycosis and chronic fungal infections. *Skin Appendage Disorders*, 4(3), 136–140.

Gupta, A.K., Mays, R.R., Versteeg, S.G., Shear, N.H. & Piguet, V. (2018) Update on current approaches to diagnosis and treatment of onychomycosis. *Expert Review of Anti-Infective Therapy*, 16(12), 929–938.

Gupta, A.K., Stec, N., Summerbell, R.C., Shear, N.H., Piguet, V., Tosti, A. et al. (2020) Onychomycosis: a review. *Journal of the European Academy of Dermatology and Venereology*, 34(9), 1972–1990.

Gupta, A.K., Versteeg, S.G., Shear, N.H., Piguet, V., Tosti, A. & Piraccini, B.M. (2019) A practical guide to curing onychomycosis: how to maximize cure at the patient, organism, treatment, and environmental level. *American Journal of Clinical Dermatology*, 20(1), 123–133.

Joshi, T., Pundir, H. & Chandra, S. (2021) Deep-learning based re-purposing of FDA-approved drugs against *Candida albicans* dihydrofolate reductase and molecular dynamics study. *Journal of Biomolecular Structure & Dynamics*, 1–17. https://doi.org/10.1080/07391102.2021.1911851

Khazir, J., Mir, B.A., Chashoo, G., Maqbool, T., Riley, D. & Pilcher, L. (2020) Design, synthesis, and anticancer evaluation of acetamide and hydrazine analogues of pyrimidine. *Journal of Heterocyclic Chemistry*, 57(3), 1306–1318.

Kukhar, Y., Smagulova, A., Daniyarova, A., Baiduissenova, A. & Kiyan, V. (2020) *Candida parapsilosis* as a causative agent of onychomycosis in patient with cirrhosis of the liver. *Journal of Fungi*, 6(313), 1–6.

Kwasny, S.M. & Opperman, T.J. (2010) Static biofilm cultures of Gram-positive pathogens grown in a microtiter format used for anti-biofilm drug discovery. *Current Protocols in Pharmacology*, 50(1), 13A–18A.

Lewis, R.E., Diekema, D.J., Messer, S.A., Pfaller, M.A. & Klepser, M.E. (2002) Comparison of E-test, chequerboard dilution and time-kill studies for the detection of synergy or antagonism between antifungal agents tested against *Candida* species. *The Journal of Antimicrobial Chemotherapy*, 49, 345–351.

Lipner, S.R., & Scher, R.K. (2019) Onychomycosis: clinical overview and diagnosis. *Journal of the American Academy of Dermatology*, 80(4), 835–851.

Liu, G., Liu, F., Huang, H.Y., Shi, S., Zhang, Y.C., Yin, Z.Y. et al. (2019) Synthesis and antifungal activities of biquinazolinediselenides compounds. *Afinidad*, 76(586), 151–157.

Lohse, M.B., Gulati, M., Craik, C.S., Johnson, A.D. & Nobile, C.J. (2020) Combination of antifungal drugs and protease inhibitors prevent *Candida albicans* biofilm formation and disrupt mature biofilms. *Frontiers in Microbiology*, 11, 1027.

Marc, W., Andrew, J.H., David, S., Karl, D.H., Lee, F.K., David, P.B. et al. (1997) X-ray crystallographic studies of *Candida albicans* dihydrofolate reductase. *International Journal of Biological Chemistry*, 272(48), 30289–30298.

Melo, T.R., Cordeiro, L.V., Souza, H.D.D.S., De Athayde-Filho, P.F., De Oliveira-Filho, A.A., Ferreira, S.B. et al. (2020) Antifungal and antibiofilm activity of 2-bromo-*N*-phenylcetamide against *Cryptococcus neoformans*. *Asian Journal of Pharmaceutical and Clinical Research*, 13(12), 173–176.

Nett, J.E. & Andes, D.R. (2020) Contributions of the biofilm matrix to *Candida* pathogenesis. *Journal of Fungi*, 6(1), 1–9.

Onsare, J.G. & Arora, D.S. (2014) Antibiofilm potential of flavonoids extracted from Moringa oleifera seed coat against *Staphylococcus aureus*, *Pseudomonas aeruginosa* and *Candida albicans*. *Journal of Applied Microbiology*, 118, 313–325.

Paškevičius, A., Švedienė, J., Kiverytė, S., Bridžiuvienė, D., Vaitonis, G. & Jablonskienė, V. (2020) *Candida* distribution in onychomycosis and *in vitro* susceptibility to antifungal agents. *Acta Dermatovenerologica Croatica*, 28(4), 204–209.

Pinzi, L. & Rastelli, G. (2019) Molecular docking: shifting paradigms in drug discovery. *International Journal of Molecular Sciences*, 20(18), 4331.

Rajasekharan, S.K., Ramesh, S., Satish, A.S. & Lee, J. (2017) Antibiofilm and anti-β- lactamase activities of burdock root extract and chlorogenic acid against *Klebsiella pneumoniae*. *Journal of Microbiology and Biotechnology*, 27(3), 542–551.

Sanad, S.M., Mekky, A.E. & El-Idreesy, T.T. (2021) Potential bacterial biofilm, MRSA, and inhibitors based on new morpholine-linked chromene-thiazole hybrids: one-post synthesis and *in silico* study. *Journal of Molecular Structure*, 1248, 131476.

Shinde, R.R., Gaikwad, D. & Farooqui, M. (2020) Synthesis and antimicrobial activity of 2-(4-(benzo [d] thiazol-5-ylsulfonyl) piperazine-1-yl)-N-substituted acetamide derivatives. *Journal of Heterocyclic Chemistry*, 57(11), 3907–3917.

Silva, D., Diniz-Neto, H., Cordeiro, L., Silva-Neta, M., Silva, S., Andrade-Júnior, F. et al. (2020) (R)-(+)-β-Citronellol and (S)-(−)-β-citronellol in combination with amphotericin B against *Candida* spp. *International Journal of Molecular Sciences*, 21(5), 1785.

Silva, D.R., Sardi, J.D.C.O., Freires, I.A., Silva, A.C.B. & Rosalen, P.L. (2019) *In silico* approaches for screening molecular targets in *Candida albicans*: a proteomic insight into drug discovery and development. *European Journal of Pharmacology*, 842, 64–69.

Silva, K.V., Lima, M.I., Cardoso, G.N., Santos, A.S., Silva, G.S. & Pereira, F.O. (2017) Inibitory effects of linalool on fungal pathogenicity of clinical isolates of Microsporumcanis and Microsporumgypseum. *Mycoses*, 60(6), 387–393.

Silva, S., Negri, M., Henriques, M., Oliveira, R., Williams, D.W. & Azeredo, J. (2011) Adherence and biofilm formation of non-*Candida albicans Candida* species. *Trends in Microbiology*, 19(5), 241–247.

Souza, H.D., de Sousa, R.P., Lira, B.F., Vilela, R.F., Borges, N.H., Siqueira-Junior, J.P.D. et al. (2019) Synthesis, *in silico* study and antimicrobial evaluation of new selenoglycolicamides. *Journal of the Brazilian Chemical Society*, 30, 188–197.

Soyer, Z. & Eraç, B. (2007) Evaluation of antimicrobial activities of some 2 (3H)-benzoxazolone derivatives. *Fabad Journal of Pharmaceutical Sciences*, 32(4), 167.

Sun, Q., Xiong, K., Yuan, Y., Yu, J., Yang, L., Shen, C. et al. (2020) Inhibiting fungal echinocandin resistance by small-molecule disruption of geranylgeranyltransferase type I activity. *Antimicrobial Agents and Chemotherapy*, 64(2), 02046-19.

Thomsen, R. & Christensen, M.H. (2006) MolDock: a new technique for high-accuracy molecular docking. *Journal of Medicinal Chemistry*, 49, 3315–3321.

Torres-Guerrero, E. & Arenas, R. (2017) *Candida* onychomycosis. In: Tosti, A., Vlahovic, T. & Arenas, R. (Eds.) *Onychomycosis*. Cham: Springer.

Vila, T.V.M., Quintanilha, N.S. & Rozental, S. (2015) Miltefosine is effective against *Candida albicans* and *Fusarium oxysporum* nail biofilms *in vitro*. *Journal of Medical Microbiology*, 64(11), 1436–1449.

Vila, T.V.M., Rozental, S. & De Sá Guimarães, C.M.D. (2015) A new model of *in vitro* fungal biofilms formed on human nail fragments allows reliable testing of laser and light therapies against onychomycosis. *Lasers in Medical Science*, 30(3), 1031–1039.

Whitlow, M., Howard, A.J., Stewart, D., Hardman, K.D., Kuyper, L.F., Baccanari, D.P. et al. (1997) X-ray crystallographic studies of *Candida albicans* dihydrofolate reductase: high resolution structures of the holoenzyme and an inhibited ternary complex. *The Journal of Biological Chemistry*, 272(48), 30289–30298.

Yadav, S., Lim, S.M., Ramasamy, K., Vasudevan, M., Ali Shan, A.S., Mathur, A. et al. (2018) Synthesis and evaluation of antimicrobial, antitubercular and anticancer activities of 2-(1-benzoyl-1*H*-benzo[*d*]imidazol-2-ylthio)-*N*-substituted acetamides. *Chemistry Central Journal*, 12(1), 1–14.

Yurttaş, L., Kubilay, A., Evren, A.E., Kısacık, İ. & Karaca Gençer, H. (2020) Synthesis of some novel 3, 4, 5-trisubstituted Triazole derivatives bearing quinoline ring and evaluation of their antimicrobial activity. *Phosphorus, Sulfur and Silicon and the Related Elements*, 195(9), 767–773.